

# Optical and Electrical Properties of Mo-doped Zr:ZnO Multilayer Thin Films for Photosensor Applications

Ming-Yu Yen,<sup>1</sup> Tao-Hsing Chen,<sup>2\*</sup> Po-Hsun Lai,<sup>2</sup>  
Sheng-Lung Tu,<sup>1</sup> and Yun-Hwei Shen<sup>1</sup>

<sup>1</sup>Department of Resources Engineering, National Cheng Kung University, Tainan City 701, Taiwan  
<sup>2</sup>Department of Mechanical Engineering, National Kaohsiung University of Science and Technology,  
Kaohsiung City 807, Taiwan

(Received October 26, 2021; accepted December 13, 2021; online published March 22, 2022)

**Keywords:** Zr:ZnO, molybdenum, multilayer films, radio-frequency magnetron sputtering, vacuum annealing

We investigated the structural, optical, and electrical properties of molybdenum and zirconium-doped zinc oxide (ZZO) with a purity of 99.99% deposited on a glass substrate by radio-frequency magnetron sputtering and annealed at different temperatures. The doping amount of zirconium on ZnO was 3 wt%. The optimal resistivity of the multilayers,  $5.1 \times 10^{-3} \Omega\text{-cm}$ , was observed for an annealing temperature of 400 °C. This film also had the highest transmittance of 93%. Moreover, the optimal figure of merit,  $4.6 \times 10^{-6} \Omega^{-1}$ , was observed for an annealing temperature of 400 °C. Furthermore, the grain size also increased with the annealing temperature, as observed by scanning electron microscopy. Mo/ZZO multilayer thin films with such excellent optical and electrical properties can be applied in photosensors.

## 1. Introduction

Transparent conductive oxide (TCO) thin films have excellent conductivity and high optical transmittance in the visible and near-IR regions. These characteristics make TCO thin films usable in various optoelectronic components, including solar cells, organic light-emitting devices, thin-film transistors, photovoltaic cells, electrochromic devices, and flat panel displays.<sup>(1–10)</sup> In general, metal films are opaque in the visible light region. However, metal films with a thickness less than 100 Å can be penetrated by visible light and exhibit strong reflectivity in the IR region. To form a semiconductor, materials with an energy gap higher than 3 eV must be used. Indium oxide, zinc oxide (ZnO), tin oxide, titanium oxide, and cadmium oxide<sup>(11)</sup> can all be used to form semiconductors. To achieve higher conductivity and transmittance, many studies have proposed combining oxide and metal films to create a multilayer structure of oxide–metal–oxide or metal oxide–metal–metal oxide transparent conductive films.<sup>(12–16)</sup> Such films can inhibit reflection from the metal layer in the visible light region and achieve light transmission.<sup>(17)</sup> In this study, we used magnetron sputtering to deposit Mo metal and ZnO:ZrO<sub>2</sub>

---

\*Corresponding author: e-mail: [thchen@nkust.edu.tw](mailto:thchen@nkust.edu.tw)  
<https://doi.org/10.18494/SAM3713>

(3 wt%) (ZZO) thin films, and produce Mo/ZZO multilayer thin films. After optimal single-layer parameters were determined, the intermediate metal layer of Mo was examined. The multilayer structure of Mo/ZZO was annealed at various temperatures to optimize the ideal electrical and optical properties. Our results suggest that the Mo/ZZO multilayer thin films can be applied in photosensors and gas sensors.

## 2. Experimental Principle and Method

We used Corning glass as the substrate. The glass substrate was cut to an appropriate size, and the cut test specimens were washed in an ultrasonic oscillator with organic solvents (deionized water, acetone, and isopropanol) and deionized water, baked in an oven (90 °C for 1 h) to remove moisture, and finally divided. Sputtering was performed using a magnetron sputtering system and argon was introduced to set the required parameters. The following conditions were used to produce multiple Mo/ZZO thin films through sputtering deposition: a bias voltage of 4 mTorr, a gas flow rate of 15 sccm using argon gas, a sputtering power of 80 W and a deposition time of 45 min for ZZO, and a sputtering power of 20 W and a deposition time of 1 min for Mo. The subsequent vacuum annealing was performed at a temperature of 200–400 °C. The crystal structure was examined by X-ray diffraction (XRD, SIEMENS D-500) with Cu-K $\alpha$  radiation. The optical transmittance properties of the films were investigated using a UV–vis spectrophotometer (Hitachi 2900). The electrical properties were determined by Hall effect measurements (AHM-800B). The surface features of the films were characterized by scanning electron microscopy (SEM, JSM-7000F), and atomic force microscopy (AFM) was used to investigate the roughness and grain size.

## 3. Results and Discussion

### 3.1 XRD properties of the annealed thin films

Figure 1 presents the XRD spectra of the Zr:ZnO thin films deposited on the Mo metal layer. From the figure, it can be seen that the multilayer films present the (002) peak for the ZnO thin film.<sup>(18,19)</sup> Furthermore, a (440) peak was also observed, and the peak intensity increased with the annealing temperature. This is because the Mo metal directly replaces the ZnO layers during annealing to form a ZnMoO<sub>3</sub> structure oriented in the secondary direction.<sup>(20)</sup> The doping during vacuum annealing can be observed from the peak shift. When the annealing temperature increases, all peaks undergo a shift, indicating the doping of large atoms; because the atomic radius of Mo (139 pm) is larger than those of Zn (134 pm) and O (60 pm), a peak shift occurs during doping.

### 3.2 Comparison of electrical properties of annealed thin films

Table 1 presents the electrical properties of Mo-doped multilayer thin films for different annealing temperatures. From the table, it can be seen that the resistivity decreases with

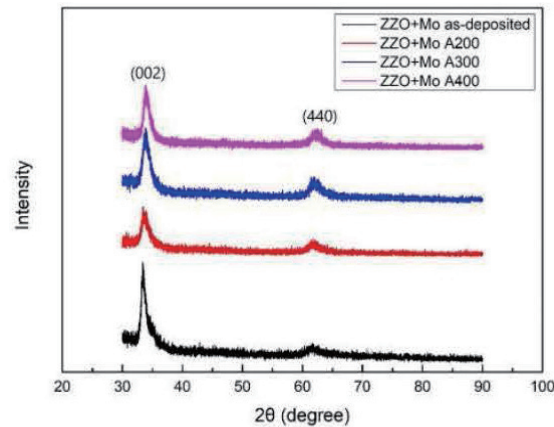


Fig. 1. (Color online) XRD spectra of Mo/ZZO for different annealing temperatures.

Table 1

Electrical properties of Mo/ZZO multilayer thin films for different annealing temperatures.

Mo (20 W, 1 min)/ZZO (80 W, 45 min)			
Annealing temperature (°C)	Resistivity ( $\Omega\text{-cm}$ )	Mobility ( $\text{cm}^2/\text{Vs}$ )	Carrier concentration ( $\text{cm}^{-3}$ )
as-deposited	$3.81 \times 10^{-2}$	$1.24 \times 10^1$	$1.3 \times 10^{19}$
200	$1.07 \times 10^{-2}$	$2.92 \times 10^1$	$3.8 \times 10^{19}$
300	$8.43 \times 10^{-3}$	$3.2 \times 10^1$	$4.8 \times 10^{19}$
400	$5.1 \times 10^{-3}$	$3.8 \times 10^1$	$5.7 \times 10^{19}$

increasing annealing temperature. The lowest resistivity is  $5.1 \times 10^{-3} \Omega\text{-cm}$  for the Mo/ZZO multilayer thin film annealed at 400 °C. This decrease in resistivity was caused by the considerable increase in the number of valence electrons in the film after annealing, which resulted in a large number of collisions during conduction.<sup>(21)</sup>

### 3.3 Comparison of optical properties of thin films after annealing

Figure 2 presents the changes in the optical properties and energy gap of the multilayer thin films after annealing. The average transmittance increased with the annealing temperature. The highest transmittance was 93% at the annealing temperature of 400 °C. The main reason for this is that sufficient valence energy was obtained in the film during annealing, but the replacement between atoms, i.e., doping, resulted in the diffusion of Mo into the oxide layer, thus reducing the mirror effect of the metal layer and increasing its transmittance. The transmittance increased considerably upon annealing at 400 °C. A possible reason for this is that the dissipation or diffusion of the metal layer into the oxide layer resulted in a discontinuity in the thin-film metal. All the Mo/ZZO multilayer thin films had a sharp absorption edge in the UV range of 300–400 nm. Because optical absorption is due to electron transitions from the valence band to the conduction band, the band gap ( $E_g$ ) was determined by the extrapolation of the straight region of

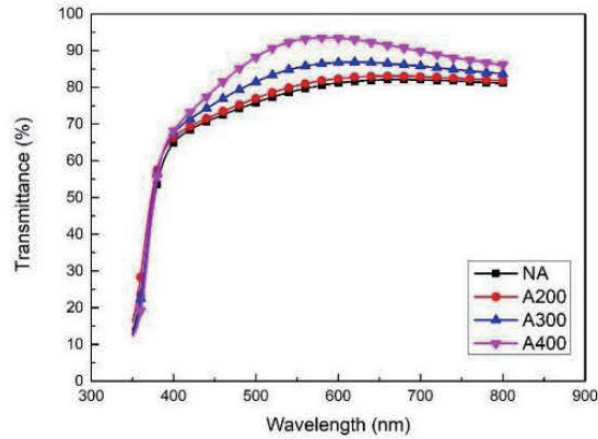


Fig. 2. (Color online) Optical transmittance of ZZO thin films for different annealing temperatures.

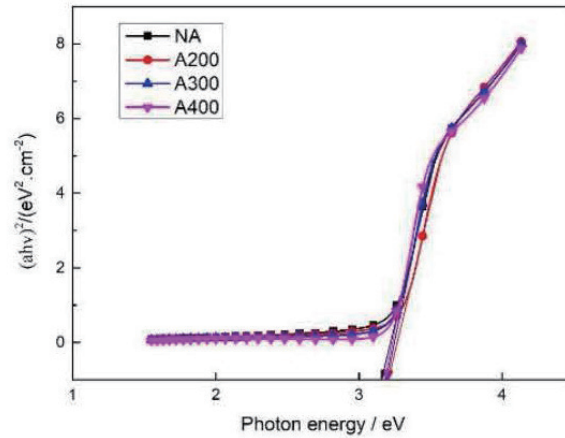


Fig. 3. (Color online) Energy gap of Mo/ZZO for different annealing temperatures.

the plot of the square of the absorption coefficient  $(ah\nu)^2$  versus photon energy  $(h\nu)$ . The energy gap can be calculated using the following optical band gap formula:<sup>(22–24)</sup>

$$(ah\nu)^2 = A(h\nu - E_g), \quad (1)$$

where  $h$  is Planck's constant,  $\nu$  is the frequency of incident photons, and  $A$  is an energy-independent constant. Figure 3 shows the variation of the absorption coefficient  $(ah\nu)^2$  for Mo/ZZO multilayer thin films plotted against the photon energy for different annealing temperatures. It can be seen that  $E_g$  initially increases from 3.15 to 3.24 eV (see Table 2) with the annealing temperature. Despite the changes in the transmittance and maximum absorption wavelength of the multilayer thin films with the annealing temperature, the optical properties of the multilayer thin films are generally similar to those of transparent conductive films with an optical band gap of 3.24 eV.

Table 2

Energy gap of Mo/ZZO multilayer thin films for different annealing temperatures.

Annealing temperature (°C)	Mo/ZZO
as-deposited	3.15
200	3.18
300	3.21
400	3.24

### 3.4 Surface morphology analysis of annealed thin films

The surface morphology of the multilayer thin films under different annealing temperatures was analyzed by AFM. The results are presented using 3D diagrams, from which their  $R_a$  values (average roughness of the center line) were measured.

Table 3 and Fig. 4 present the surface morphology and roughness of the multilayer thin films for different annealing temperatures. The roughness  $R_a$  was less than 1 nm for all parameters, which indicates that the deposition of the films was uniform.  $R_a$  decreased with increasing annealing temperature, which indicates that the density of the film surface was increased by annealing.<sup>(25)</sup> For each annealing temperature, no holes or cracks were observed on the film surface, and a small change in surface morphology among the multilayer thin films was observed. Figure 4 also shows that the surface flatness increased with the annealing temperature. The surface observation can also be observed by SEM as shown in Fig. 5. From Fig. 5, it can be seen that as the annealing temperature increased to 400 °C, the surface became smooth and dense, indicating improved crystallinity; thus, the grain size increased with the annealing temperature.

Table 3

Roughness of Mo-doped multilayer thin films for different annealing temperatures.

Annealing temperature (°C)	Mo/ZZO $R_a$ (nm)
as-deposited	0.21
200	0.18
300	0.15
400	0.13

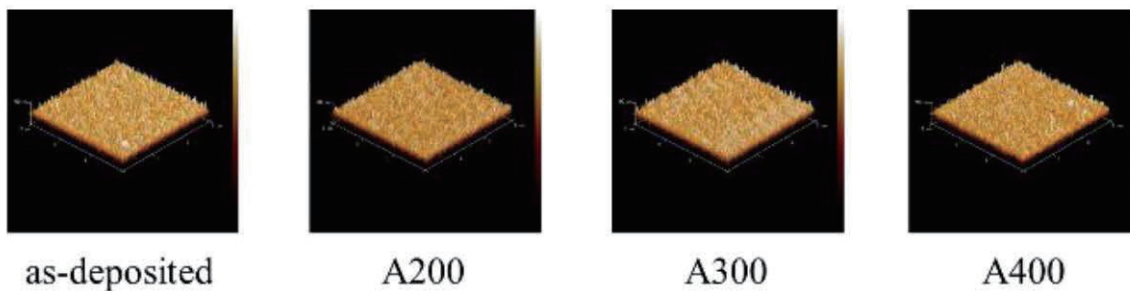


Fig. 4. (Color online) AFM images of Mo/ZZO multilayer thin films for different annealing temperatures.

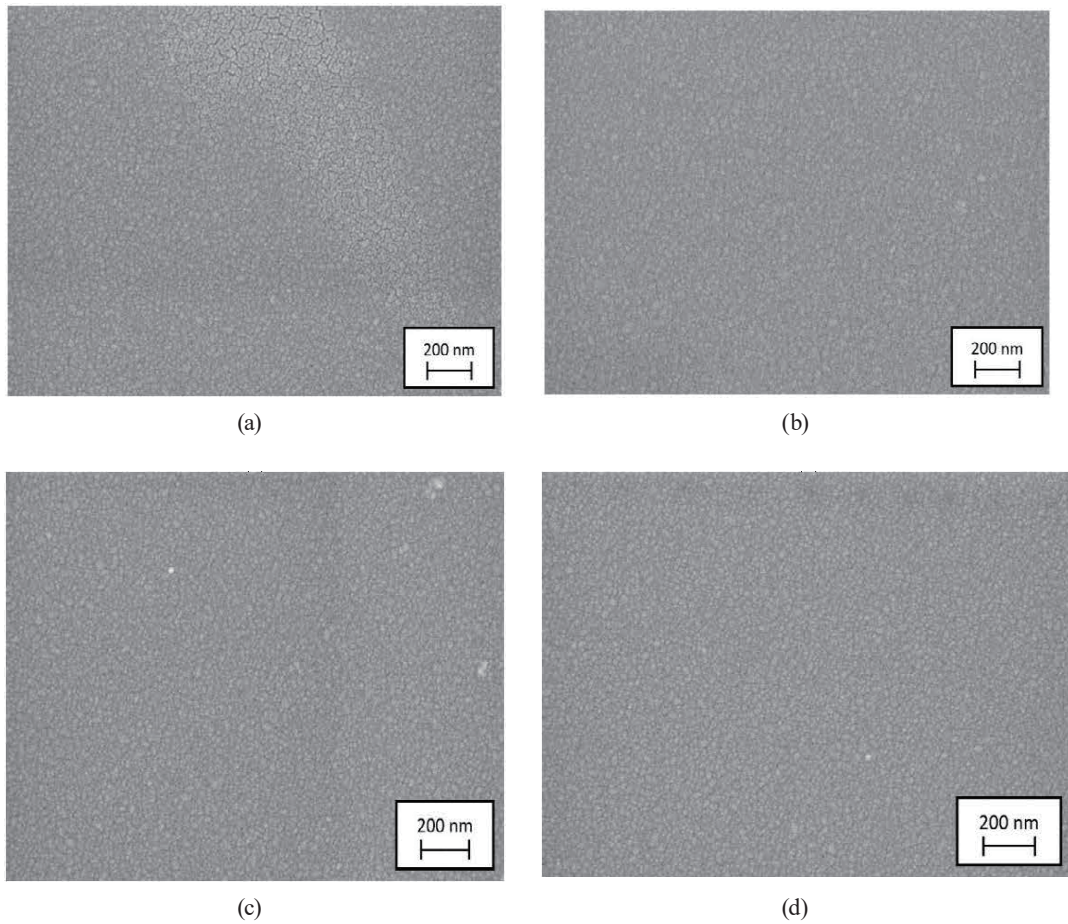


Fig. 5. (Color online) SEM images of thin film surfaces: (a) as-deposited, (b) 200 °C, (c) 300 °C, and (d) 400 °C.

### 3.5 Analysis of grain size of annealed multilayer thin films

The grain size can be calculated by substituting values measured through XRD into Scherrer's formula<sup>(26,27)</sup> to obtain the full width at half maximum (FWHM) as

$$D = \frac{0.9\lambda}{\beta \cos \theta}, \quad (2)$$

where  $D$  is the calculated grain size,  $\lambda$  is the incident wavelength,  $\theta$  is the angle of the incident ray, and  $\beta$  is the FWHM. Because  $\theta$  and  $\lambda$  are fixed values, an inverse relationship exists between  $D$  and  $\beta$ . The FWHM decreases with increasing grain size. Table 4 presents the FWHM and grain size of the Mo/ZZO multilayer thin films for different annealing temperatures. The grain size increased from 13 nm for the as-deposited sample to 21 nm for the sample annealed at 400 °C.

Table 4  
Effect of annealing temperature on grain size of Mo/ZZO multilayer films.

Annealing temperature (°C)	FWHM	Grain size (nm)
as-deposited	0.633	13
200	0.59	16
300	0.53	18
400	0.49	21

Table 5  
FOM,  $\Phi_{TC}$  ( $\Omega^{-1}$ ), of multilayer thin films for different annealing temperatures.

Annealing temperature (°C)	Mo/ZZO
as-deposited	$3.4 \times 10^{-6}$
200	$3.9 \times 10^{-6}$
300	$4.20 \times 10^{-6}$
400	$4.60 \times 10^{-6}$

### 3.6 Analysis of figure of merit of annealed thin films

The figure of merit (FOM) is the main way of determining the quality of transparent conductive films.<sup>(28)</sup> The FOM can be calculated from the transmittance and film resistivity. As shown in Eq. (3), the FOM is directly proportional to the 10th power of the transmittance. Therefore, the optical transmittance has a considerable effect on the FOM. To have high-quality transparent conductive films, both high transmittance and low resistivity are needed.

$$\Phi_{TC} = \frac{T_{av}^{10}}{R_{sh}} \quad (3)$$

Table 5 presents the FOM of the multilayer thin films. The optimal FOM was observed for the multilayer thin film annealed at 400 °C.

## 4. Conclusions

We investigated Mo/ZZO multilayer thin films deposited on Corning glass substrates by RF magnetron sputtering. The effects of the annealing temperature on the structural, electrical, and optical properties of the Mo/ZZO multilayer thin films were investigated. When the annealing temperature was increased to 400 °C, the resistivity decreased owing to the improved crystallinity. This indicates that during sputter deposition, the metal layer was doped on the oxide layer and that the amount of doping increased after annealing. In terms of the electrical properties, the lowest resistivity ( $5.1 \times 10^{-3} \Omega\text{-cm}$ ) was observed for the annealing temperature of 400 °C. In terms of optical transmittance, the maximum average transmittance for the multilayer films was 93% for an annealing temperature of 400 °C. Furthermore, the energy gap increased slightly from 3.15 eV before annealing to 3.24 eV after annealing at 400 °C. In terms of surface morphology,  $Ra$  decreased with the annealing temperature. This means that the grain size increased with the annealing temperature, from 13 nm before annealing to 21 nm after annealing at 400 °C. To achieve high FOM, a film must have good balance between optical and electrical properties. The optimal FOM of  $4.6 \times 10^{-6} \Omega^{-1}$  was achieved when the annealing temperature of the Mo/ZZO multilayer thin film was 400 °C. Hence, Mo/ZZO multilayer thin films have potential use in optoelectronic sensor applications.

## Acknowledgments

This paper is a product of a research project supported by the Ministry of Science and Technology (Project No. MOST 110- 2628-E-992-002). The authors would like to express their gratitude to the Ministry of Science and Technology, the support of which enabled this research to be conducted smoothly.

## References

- 1 G. Golan and A. Axelevitch: *Microelectron. J.* **31** (2000) 469. [https://doi.org/10.1016/S0026-2692\(99\)00148-2](https://doi.org/10.1016/S0026-2692(99)00148-2)
- 2 P. Misra, V. Ganeshan, and N. Agrawal: *J. Alloy Compd.* **725** (2017) 60. <https://doi.org/10.1016/j.jallcom.2017.07.121>
- 3 K. Fleischer, E. Arca, and I. V. Shvets: *Sol. Energy Mater. Sol. Cells* **101** (2012) 262. <https://doi.org/10.1016/j.solmat.2012.01.037>
- 4 M. Nisha, S. Anusha, A. Antony, R. Manoj, and M. K. Jayaraj: *Appl. Surf. Sci.* **252** (2005) 1430. <https://doi.org/10.1016/j.apsusc.2005.02.115>
- 5 C. Li, C. Han, Y. Zhang, Z. Zang, M. Wang, X. Tang, and J. Du: *Sol. Energy Mater. Sol. Cells* **172** (2017) 341. <https://doi.org/10.1016/j.solmat.2017.08.014>
- 6 C. F. Liu, T. H. Chen, and J. T. Huang: *Sens. Mater.* **32** (2020) 3727. <https://doi.org/10.18494/SAM.2020.3138>
- 7 P. Nunes, E. Fortunato, P. Tonello, F. B. Fernandes, P. Vilarinho, and R. Martins: *Vacuum* **64** (2002) 281. [https://doi.org/10.1016/S0042-207X\(01\)00322-0](https://doi.org/10.1016/S0042-207X(01)00322-0)
- 8 T. H. Chen and H. T. Su: *Sens. Mater.* **30** (2018) 2541. <https://doi.org/10.18494/SAM.2018.2056>
- 9 T. H. Chen and C. L. Yang: *Opt. Quantum Electron.* **48** (2016) 533. <https://doi.org/10.1007/s11082-016-0808-3>
- 10 T. H. Chen and T. Y. Chen: *Nanomaterials* **5** (2015) 1831. <https://doi.org/10.3390/nano5041831>
- 11 E. Shanthi, A. Banerjee, V. Dutta, and K. L. Chopra: *J. Appl. Phys.* **53** (1982) 1615. <https://doi.org/10.1063/1.330619>
- 12 K. P. Sibin, N. Selvakumar, A. Kumar, A. R. Dey, N. Sridhara, H. D. Shashikala, A. K. Sharma, and H. C. Barshilia: *Sol. Energy* **141** (2017) 118. <https://doi.org/10.1016/j.solener.2016.11.027>
- 13 B. Sarma and B. K. Sarma: *J. Alloy Compd.* **734** (2018) 210. <https://doi.org/10.1016/j.jallcom.2017.11.028>
- 14 D. R. Sahu, S. Y. Lin, and J. L. Huang: *Thin Solid Films* **516** (2008) 4728. <https://doi.org/10.1016/j.tsf.2007.08.089>
- 15 Y. Guo, W. Cheng, J. Jiang, S. Zuo, F. Shi, and J. Chu: *Vacuum* **131** (2016) 164. <https://doi.org/10.1016/j.vacuum.2016.06.014>
- 16 D. R. Sahu, S. Y. Lin, and J. L. Huang: *Appl. Surf. Sci.* **252** (2006) 7509. <https://doi.org/10.1016/j.apsusc.2005.09.021>
- 17 J. C. Fan, F. J. Bachner, G. H. Foley, and P. M. Zavracky: *Appl. Phys. Lett.* **25** (1974) 693. <https://doi.org/10.1063/1.1655364>
- 18 N. E. Sung, M. A. Marcus, K. S. Lee, H. J. Yun, and I. J. Lee: *Thin Solid Films* **696** (2020) 137782. <https://doi.org/10.1016/j.tsf.2019.137782>
- 19 H. Zhang, H. Liu, and L. Feng: *Vacuum* **84** (2010) 833. <https://doi.org/10.1016/j.vacuum.2009.11.005>
- 20 T. Ghrib, A. L. Al-Otaibi, M. Alqahtani, N. A. Altamimi, A. Bardaoui, and S. Brini: *Sens. Actuators, A* **297** (2019) 11537. <https://doi.org/10.1016/j.sna.2019.111537>
- 21 B. H. Choi and H. B. Im: *Thin Solid Films* **193/194** (1990) 712. [https://doi.org/10.1016/0040-6090\(90\)90223-Z](https://doi.org/10.1016/0040-6090(90)90223-Z)
- 22 N. E. Sung, K. S. Lee, and I. J. Lee: *Thin Solid Films* **651** (2018) 42. <https://doi.org/10.1016/j.tsf.2018.02.011>
- 23 J. Tauc, R. Grigorovici, and A. Vancu: *Phys. Status Solidi B* **15** (1966) 627. <https://doi.org/10.1002/pssb.19660150224>
- 24 S. Venkatachalam, Y. Iida, and Y. Kanno: *Superlattices Microstruct.* **44** (2008) 127. <https://doi.org/10.1016/j.spmi.2008.03.006>
- 25 V. Gokulakrishnan, S. Parthiban, K. Jeganathan, and K. Ramamurthi: *Appl. Surf. Sci.* **257** (2011) 9068. <https://doi.org/10.1016/j.apsusc.2011.05.102>
- 26 M. Caglar, S. Ilican, and Y. Caglar: *Thin Solid Films* **517** (2009) 5023. <https://doi.org/10.1016/j.tsf.2009.03.037>
- 27 M. Lv, X. Xiu, Z. Pang, Y. Dai, L. Ye, C. Cheng, and S. Han: *Thin Solid Films* **516** (2008) 2017. <https://doi.org/10.1016/j.tsf.2007.06.173>
- 28 G. Haacke: *J. Appl. Phys.* **47** (1976) 4086. <https://doi.org/10.1063/1.323240>

## About the Authors



**Ming-Yu Yen** graduated from National Sun Yat-sen University with an EMBA in 2015. He has been studying on the human resource management Ph.D. program of National Sun Yat-sen University and the resources engineering Ph.D. program of National Chen Kung University since 2015 and 2017, respectively.



**Tao-Hsing Chen** received his B.S. degree from National Cheng Kung University, Taiwan, in 1999 and his M.S. and Ph.D. degrees from the Department of Mechanical Engineering, National Cheng Kung University in 2001 and 2008, respectively. From 2008 to 2010, he was a postdoctoral researcher at the Center for Micro/Nano Science and Technology, National Cheng Kung University. In 2010, he became an assistant professor at National Kaohsiung University of Applied Sciences (renamed National Kaohsiung University of Science and Technology), Taiwan. Since 2016, he has been a professor at National Kaohsiung University of Science and Technology. His research interests are in metal materials, TCO thin films, thermal sensors, and photosensors. ([thchen@nkust.edu.tw](mailto:thchen@nkust.edu.tw))



**Po-Hsun Lai** received his B.S. degree from National Kaohsiung University of Science and Technology, Taiwan, where he is currently studying toward his M.S. degree. His research interests are in MEMS, materials engineering, and sensors.



**Sheng-Lung Tu** received his M.S. degree from the Department of Mechanical Engineering, National Cheng Kung University in 2010 and his Ph.D. degree from the Department of Resources Engineering, National Cheng Kung University in 2014. Since 2014, he worked in general affairs at National Cheng Kung University. His research interests are in PVD technology, thin-film technology, and sensors.



**Yun-Hwei Shen** received his B.S. degree from the Department of Mineral and Petroleum Engineering, National Cheng Kung University in 1982, his M.S. degree from the Department of Mineral Preparation Engineering, University of Alaska Fairbanks, USA, in 1987, and his Ph.D. degree from the Department of Environmental Engineering, Penn State University, USA, in 1992. Since 1999, he has been a professor at the Department of Resources Engineering, National Cheng Kung University. His research interests are in catalysis technology, the hydrometallurgical processing of resource materials, sensors, and hydrometallurgical processes.